# Secondary Structure-Induced Aggregation by Hydrogen Peroxide: A Stimuli-Triggered Open/Close Implementation by Recombination

Guiyang Zhang,[a,b] Qiaobo Liao,[a] Yanfeng Liu,[a,b] Li Wang,[a,b] Huilin Gou,[a] Can Ke,[a] Xin Huang,[a,b] Kai Xi *[a] and Xudong Jia*[a,b]

[a] Department of Polymer Science & Engineering, School of Chemistry and Chemical Engineering, Nanjing University, Nanjing 210023, P. R. China.

[b] State Key Laboratory of Coordination Chemistry, Nanjing University, Nanjing 210023, PR China

# Supporting Information

# Table of Contents

**Figure S2.** ESI-MS spectra of compound Ge -di(HMPBA-pin).

**Figure S3.** (a) TEM image of the nanorods, (b-d) HRTEM image of an individual nanorod created within 5 seconds. The inset shows the corresponding lattice fringes of the area within the dotted circle.

**Figure S4.** Schematic representation for the spherical micelles based on self-assembly of Ge-di(HMPBA-pin) and TPGS-A.

**Figure S5.** $^1$H NMR spectra of TPGS, TPGS-A.

**Figure S6.** ESI-MS spectra of TPGS (a) and TPGS-A (b).

**Figure S7.** Schematic representation for the synthesis of spherical micelles via self-assembly of Genistein and TPGS.

**Figure S8.** Schematic representation for the synthesis of nanoribbon via self-assembly of HMPBA-pin-SA and TPGS.

**Figure S9.** (a) UV-vis absorption spectra and (b) absorbance intensity ratios, $A_{637}/A_{520}$, recorded for the aqueous colorimetric assay (3 nM of AuNPs) and 1.5 μM polymer upon adding varying amount of $H_2O_2$ (0-150 equiv. relative to polymer moieties) at pH 7.4 and 25 °C. Optical visualization of the colorimetric assay (3 nM of AuNPs) and 1.5 μM polymer in the absence of $H_2O_2$ (left) and 1 h after the addition of the aqueous solution of $H_2O_2$ (100 equiv. relative to nanorod moieties) at pH 7.4 and 25 °C. (c, d) The TEM images obtained by drying the two aqueous dispersions corresponded to the insert in (a).

**Figure S10.** (a) HR TEM image of the aggregated $MoS_2$ QDs. (b) A partially destroyed micelle after the high-energy electron beam irradiation of 200 kV. The inset shows the corresponding lattice fringes of the area within the dotted circle. (c) Hydrodynamic diameter, $D_h$, distribution of dissociated the aggregated $MoS_2$ QDs in aqueous solution (0.5 mg/L).

**Figure S11**. (a) excitation-dependent PL behavior of $MoS_2$ QDs. (b) aggregated $MoS_2$ QDs under different excitation wavelengths.

**Figure S12.** $^1$H NMR spectra of TPE-CHO in $CDCl_3$.

**Figure S13.** The digital photographs of TPE on the micelles surfaces in the faint yellow powder stored at room temperature (a); (b) the blue fluorescence of TPE on the micelles surfaces under UV light ($\lambda_{ex}$ = 365 nm).

**Figure S14.** (a, b) The TEM images obtained by drying the two aqueous dispersions corresponded

to the inset in every picture at the same condition. (c) TEM image of the $Cu^{2+}$ dispersion. (d) TEM image of the aggregated micelles.

**Figure S15.** Polymer nanorod glutamate toxicity-induced cell death. Concentration-dependent effect of water soluble nanorod on HT22 cell viability alone and with 4 mM glutamate. Nanorod was added to the cell media prior to the glutamate exposure and cell viability was estimated 24 h after addition. Nanorod alone upto 30 µg had no effect on cell viability whereas glutamate exposure significantly reduced the survival of cells to nearly 30% of control. Pretreatment of cells with Nanorod resisted the effect of glutamate toxicity thereby showed significant reduction in cell mortality. Nanorod concentration of 10 µg showed maximum protection to glutamate induced cell death in HT22 cells.

**Figure S16.** Polymer nanorod glutamate toxicity-induced cell death. Representative photomicrograph of HT22 cells treated with nanorod, glutamate, genistein and both. Data are the representation of 3 or more independent experiments conducted in triplicate. Glu=glutamate, Ge=genistein, Glu + naorod=glutamate + nanorod and Glu+nanorod-10 to 30 = glutamate (4 mM) + nanorod (10-30 µg).

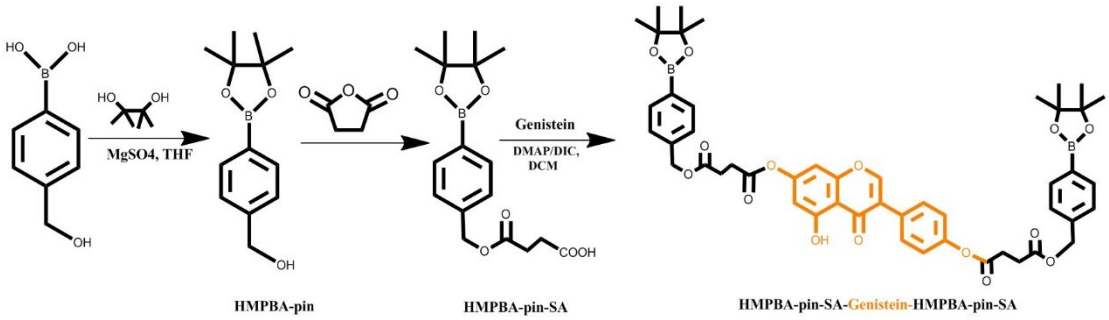


**Scheme S1.** Synthesis route of Ge-crosslinker (Ge -di(HMPBA-pin)).

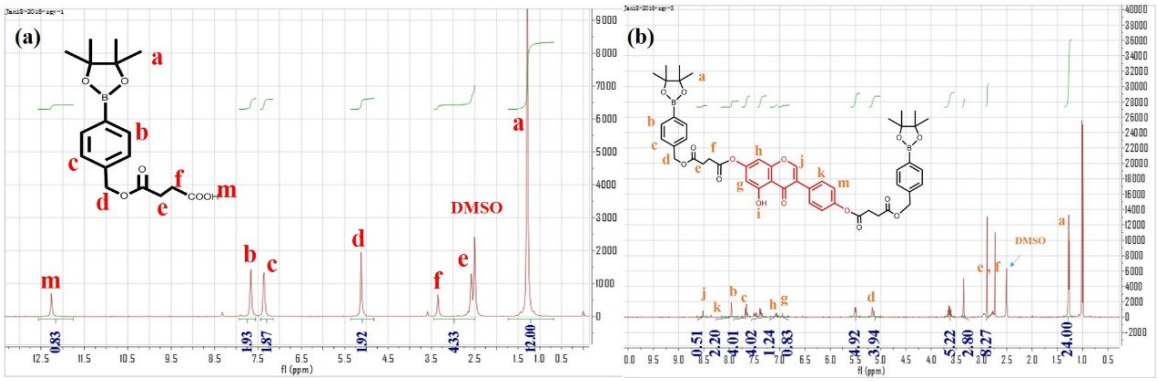

**Figure S1.** $^{1}$H NMR spectra of HMPBA-pin-SA (a) and (b) Ge -di(HMPBA-pin) in DMSO.

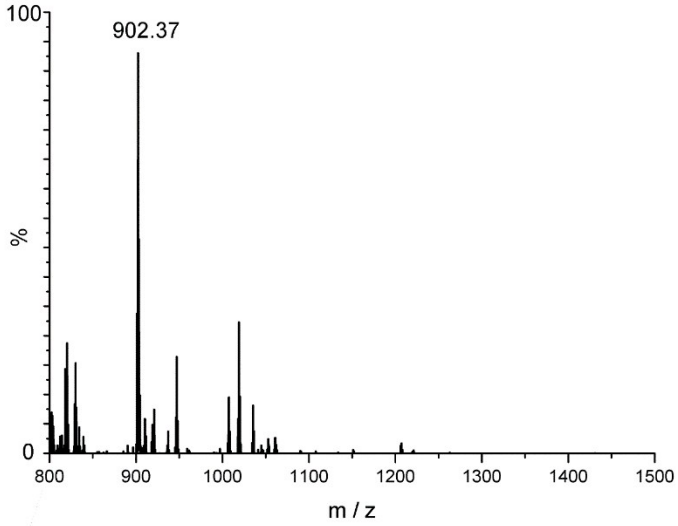


**Figure S2.** ESI-MS spectrum of compound Ge -di(HMPBA-pin).

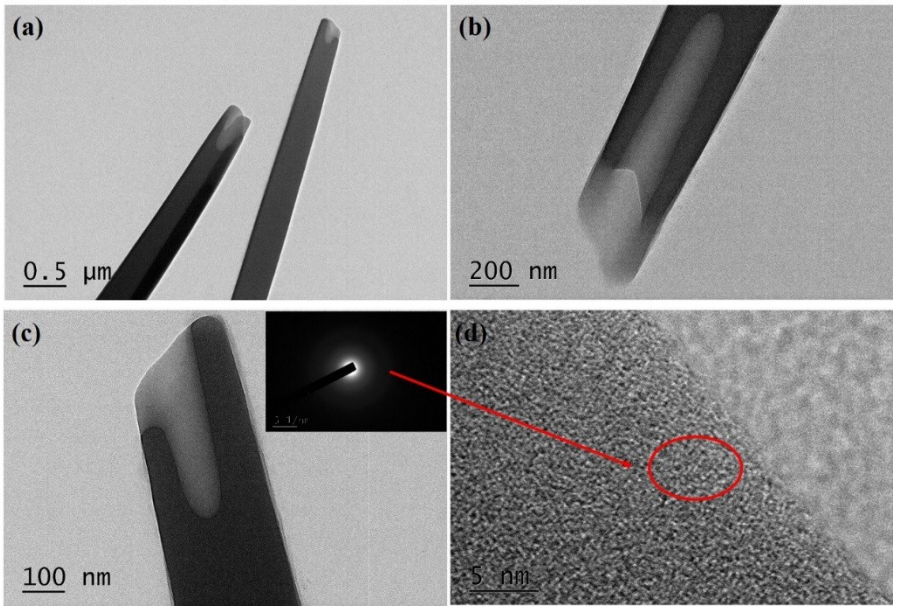


**Figure S3.** (a) TEM image of the nanorods, (b-d) HRTEM image of an individual nanorod created within 5 seconds. The inset shows the corresponding lattice fringes of the area within the dotted circle.

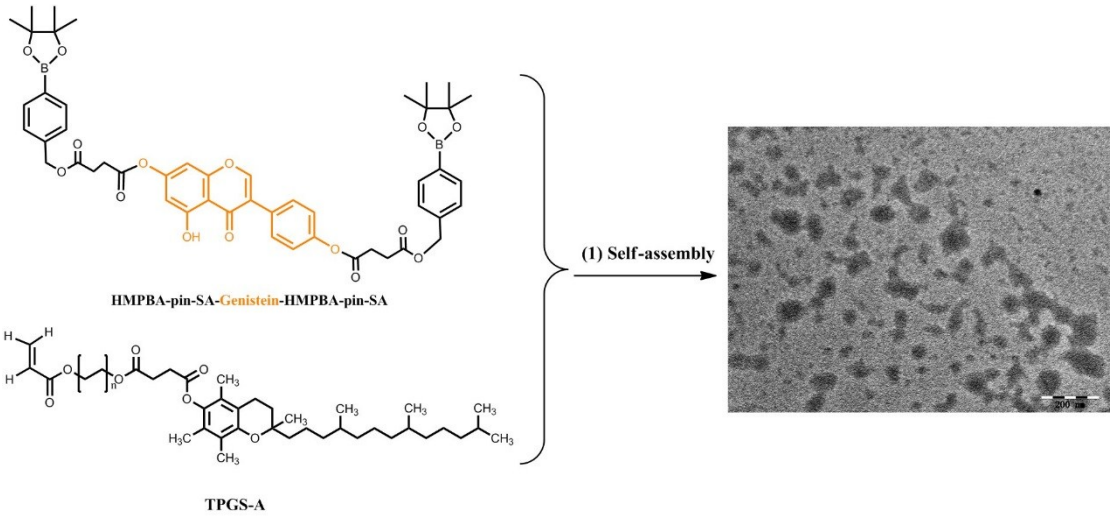


**Figure S4.** Schematic representation for the synthesis of spherical micelles via self-assembly of Ge-di(HMPBA-pin) and TPGS-A.

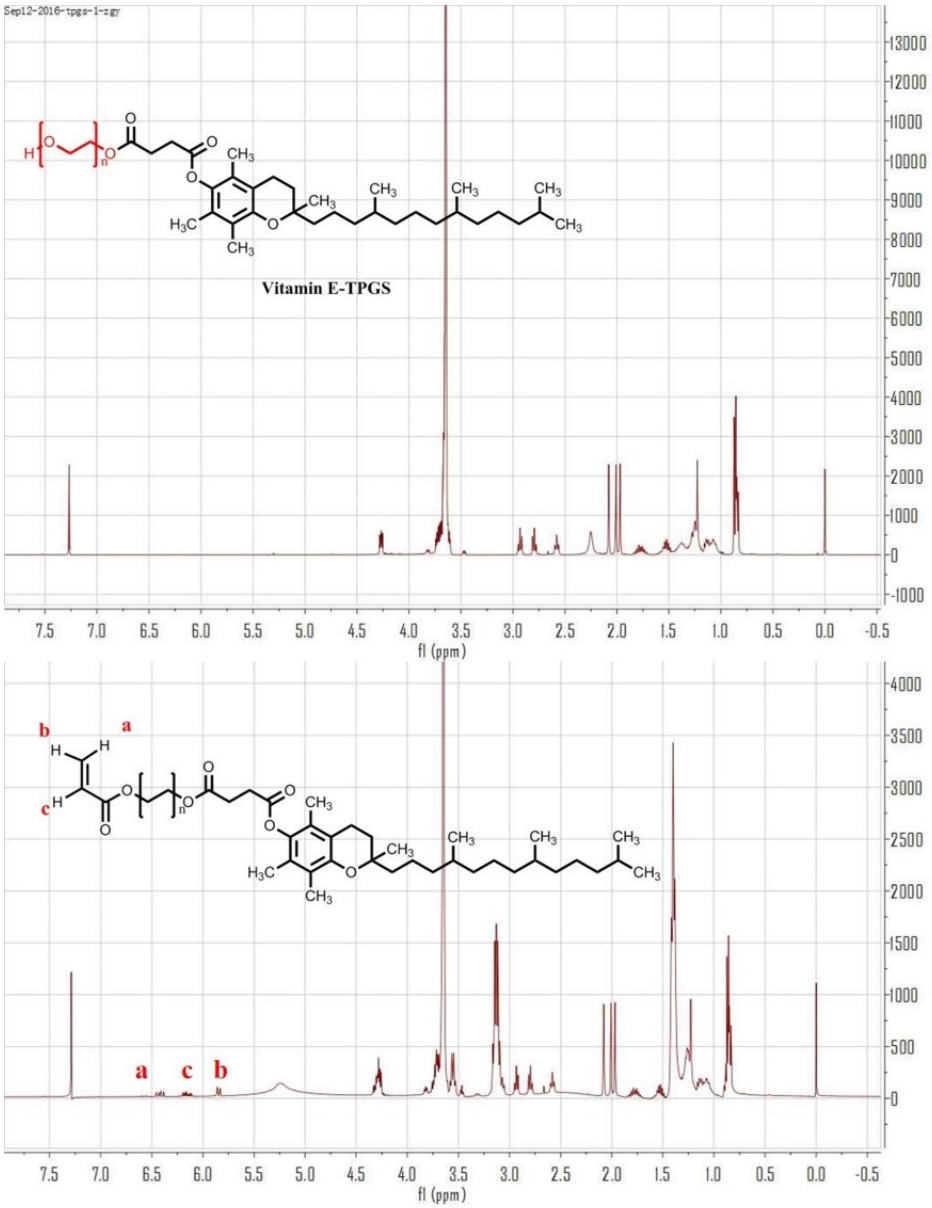


**Figure S5.** $^{1}$H NMR spectra of TPGS (top), and TPGS-A (bottom).

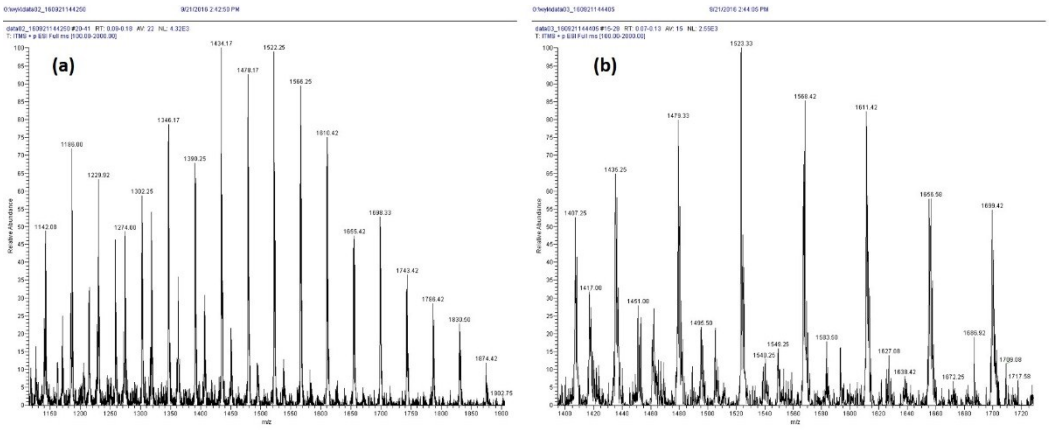


**Figure S6.** ESI-MS spectra of (a) TPGS and (b)TPGS-A.

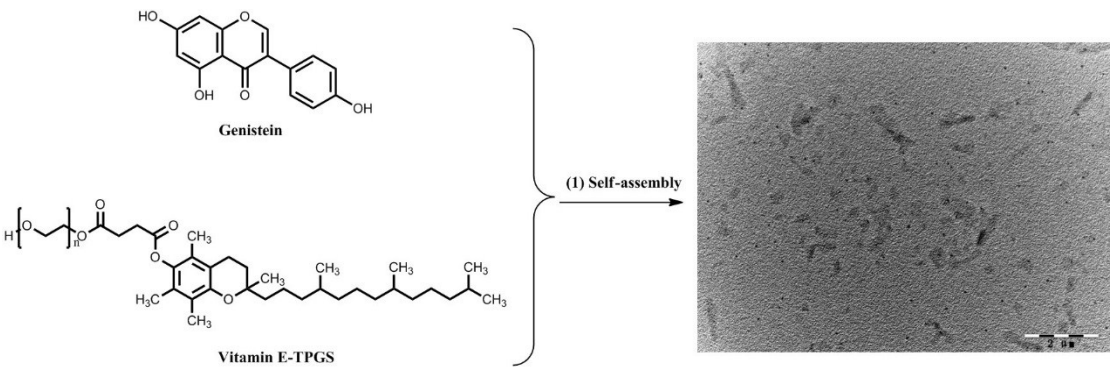


**Figure S7.** Schematic representation for the synthesis of spherical micelles via self-assembly of Genistein and TPGS.

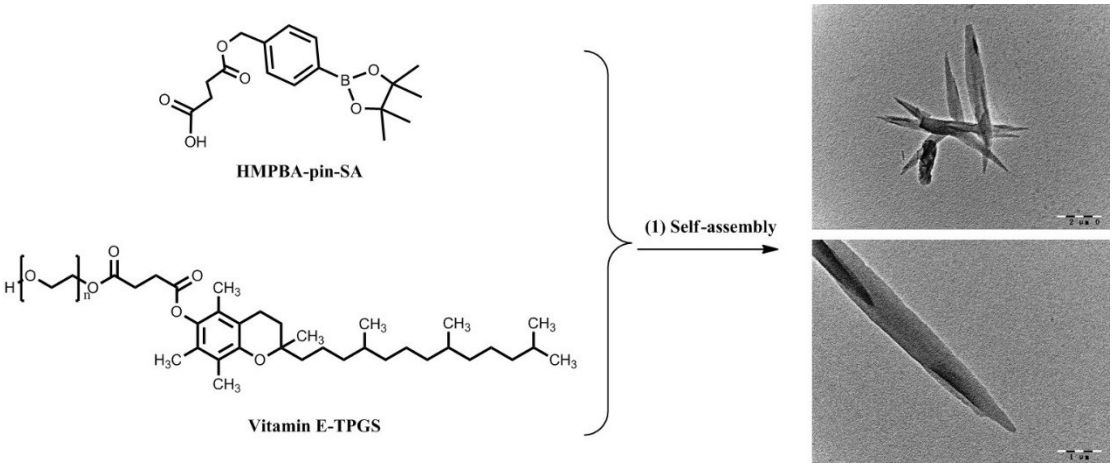


**Figure S8.** Schematic representation for the synthesis of nanoribbon via self-assembly of HMPBA-pin-SA and TPGS.

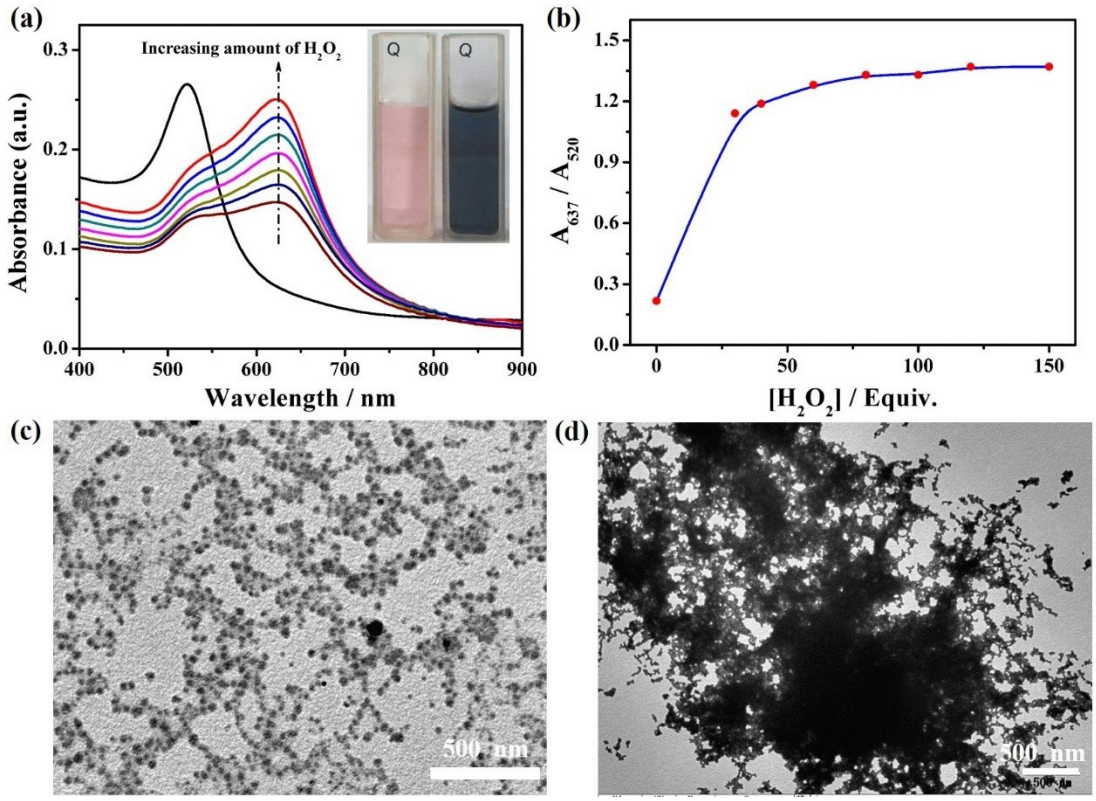


**Figure S9.** (a) UV-vis absorption spectra and (b) absorbance intensity ratios, $A_{637}/A_{520}$, recorded for the aqueous colorimetric assay (3 nM of AuNPs) and 1.5 μM polymer upon adding varying amount of $H_2O_2$ (0-150 equiv. relative to polymer moieties) at pH 7.4 and 25 °C. Optical visualization of the colorimetric assay (3 nM of AuNPs) and 1.5 μM polymer in the absence of $H_2O_2$ (left) and 1 h after the addition of the aqueous solution of $H_2O_2$ (100 equiv. relative to nanorod moieties) at pH 7.4 and 25 °C. (c, d) The TEM images obtained by drying the two aqueous dispersions corresponded to the insert in (a).

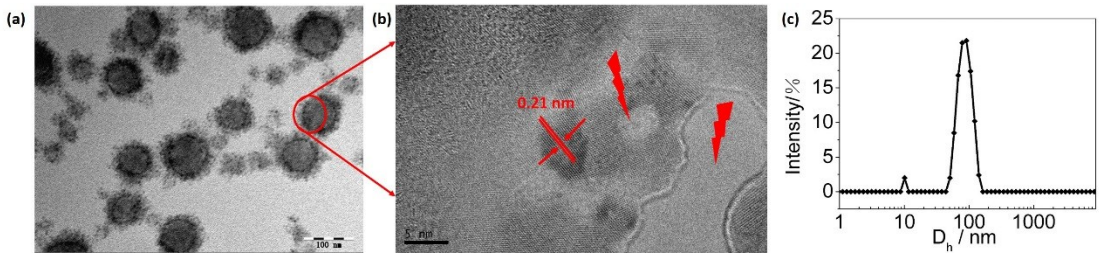


**Figure S10.** (a) HR TEM image of the aggregated $MoS_2$ QDs. (b) A partially destroyed micelle after the high-energy electron beam irradiation of 200 kV. The inset shows the corresponding lattice fringes of the area within the dotted circle. (c) Hydrodynamic diameter, $D_h$, distribution of dissociated the aggregated $MoS_2$ QDs in aqueous solution (0.5 mg/L).

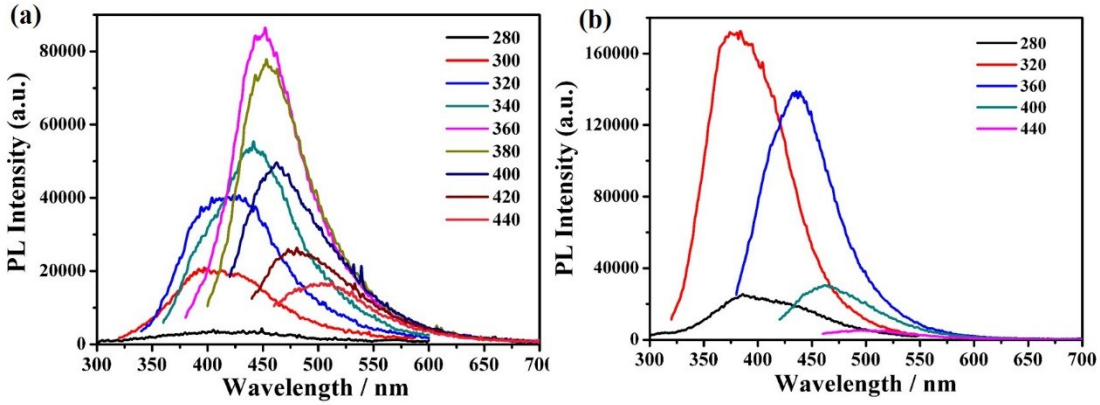


**Figure S11**. (a) excitation-dependent PL behavior of $MoS_2$ QDs. (b) aggregated $MoS_2$ QDs under different excitation wavelengths.

**Quantum Yields (QYs) Measurement**

Rhodamine B in ethanol (QY = 0.65, from literature[1] ) was selected as a control standard. The QYs of $MoS_2$ QDs and aggregated $MoS_2$ QDs were estimated according to the follow equation:

$$\Phi = \Phi_r \times \frac{I}{A} \times \frac{A_r}{I_r} \times \frac{n^2}{n_r^2}$$

Where the Φ is the QY, I is the integrated PL emission intensity (excited at 270 nm for $MoS_2$ QDs and at 285 nm for aggregated $MoS_2$ QDs, respectively), n is the refractive index (= 1.3614 for ethanol), and A is the absorbance value at the excitation wavelength of 270 nm and 285 nm in ethanol, respectively (the value of A should be less than 0.1 at the excitation wavelength). The subscript "r" refers to the standards.

**Table S1**. QYs of the $MoS_2$ QDs and aggregated $MoS_2$ QDs dispersed in ethanol.

| Samples | Integrated emission intensity (*I*) | Abs. 270 nm (*A*) | Refractive index of solvent (*n*) | QY (Φ) |
|---|---|---|---|---|
| Rhodamine B | 20255 | 0.0195 | 1.362 | 0.65 |
| $MoS_2$ QDs | 10125 | 0.0371 | 1.362 | 0.08 |
| Samples | Integrated emission intensity (*I*) | Abs. 285 nm (*A*) | Refractive index of solvent (*n*) | QY (Φ) |
| Rhodamine B | 27640 | 0.0043 | 1.362 | 0.65 |
| Self-assembly $MoS_2$ QDs | 70708 | 0.03987 | 1.362 | 0.15 |

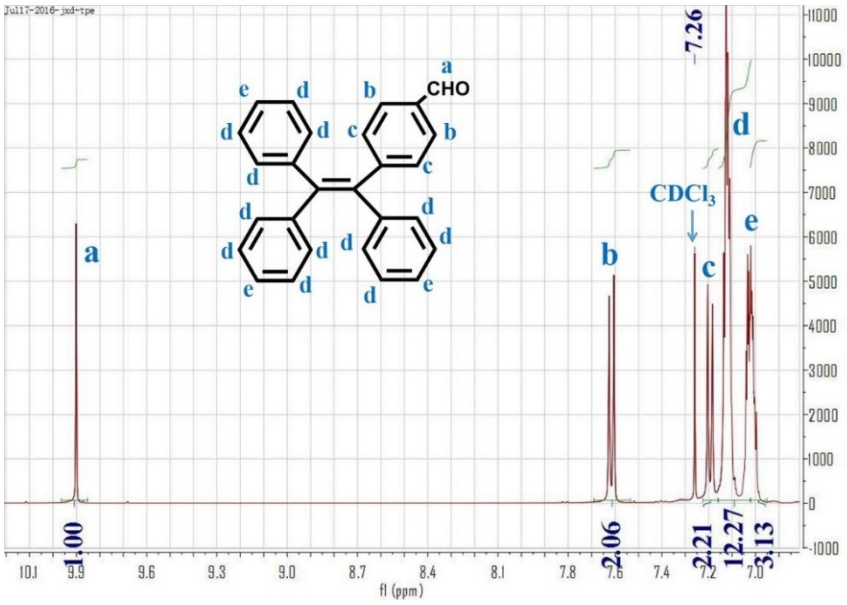


**Figure S12.** $^1$H NMR spectra of TPE-CHO in $CDCl_3$. $^1$H NMR ($CDCl_3$, 400 MHz, ppm): δ 7.02-7.03 (m, 3H), 7.11 (m, 12H), 7.18 (d, 2H), 7.60-7.63 (d, 2H), 9.90 (s, 1H).

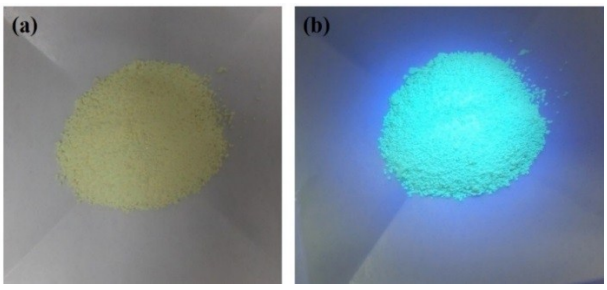


**Figure S13.** The digital photographs of (a) TPE on the micelles surfaces in the faint yellow powder stored at room temperature; (b) the blue fluorescence of TPE on the micelles surfaces under UV light ($\lambda_{ex}$ = 365 nm).

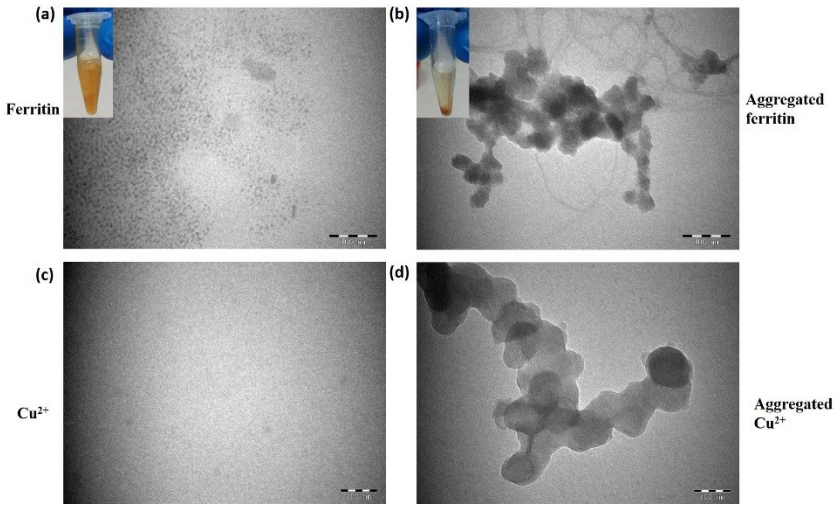


**Figure S14.** (a, b) The TEM images obtained by drying the two aqueous dispersions corresponded to the inset in every picture at the same condition. (c) TEM image of the $Cu^{2+}$ dispersion. (d) TEM image of the aggregated micelles.

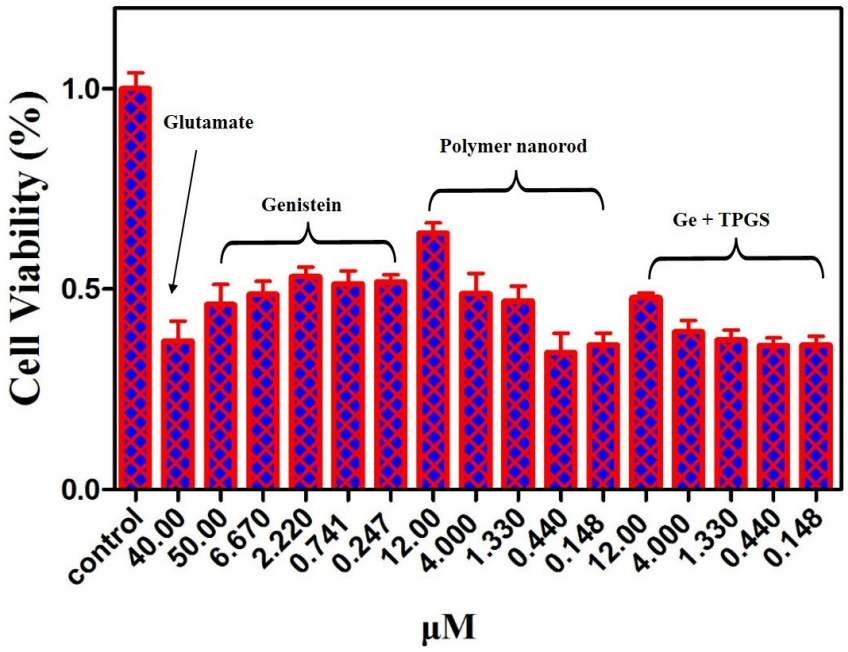


**Figure S15.** Polymer nanorod glutamate toxicity-induced cell death. Concentration-dependent effect of water soluble nanorod on HT22 cell viability alone and with 4 mM glutamate. Nanorod was added to the cell media prior to the glutamate exposure and cell viability was estimated 24 h after addition. Nanorod alone upto 30 μg had no effect on cell viability whereas glutamate exposure significantly reduced the survival of cells to nearly 30% of control. Pretreatment of cells with Nanorod resisted the effect of glutamate toxicity thereby showed significant reduction in cell mortality. Nanorod concentration of 10 μg showed maximum protection to glutamate induced cell

death in HT22 cells.

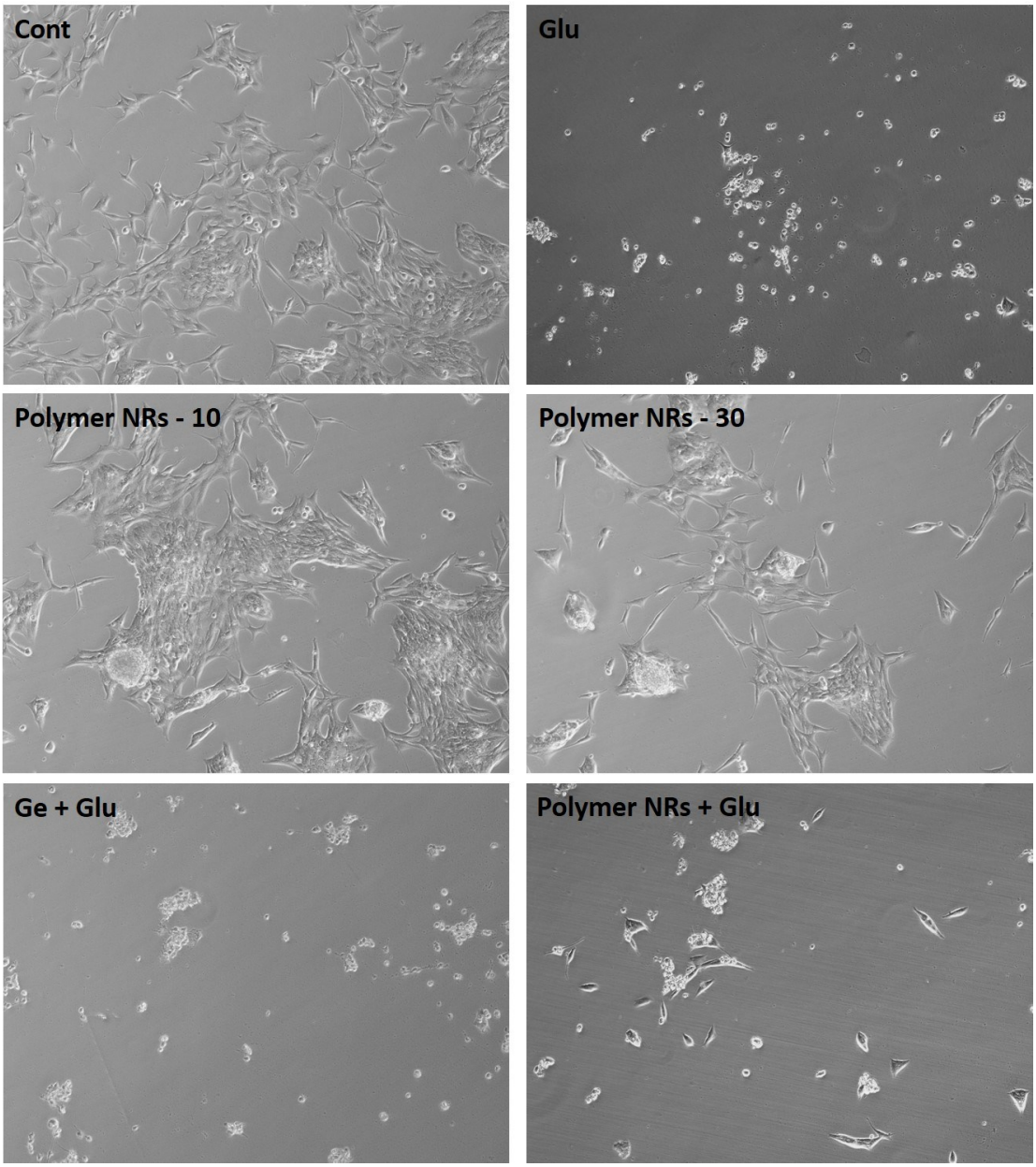


**Figure S16.** Polymer nanorod glutamate toxicity-induced cell death. Representative photomicrograph of HT22 cells treated with nanorod, glutamate, genistein and both. Data are the representation of 3 or more independent experiments conducted in triplicate. Glu=glutamate, Ge= genistein, Glu + naorod=glutamate + nanorod and Glu+nanorod-10 to 30 = glutamate (4 mM) + nanorod (10-30 μg).

**REFERENCES**

1 R. F. Kubin and A. N. Fletcher, Fluorescence quantum yields of some rhodamine dyes. *J. Lumin.*, 1982, **27**(4), 455.